

DC-to-DC Converter for Low Voltage Solar Applications

K. H. EDELMOSER, H. ERTL
 Institute of Electrical Drives and Machines
 Technical University Vienna
 Gusshausstr. 27-29, A-1040 Wien
 AUSTRIA

Abstract: - Ultra low input voltage range (several volts) DC-to-DC converters with a respectively high output voltage span have, due to the high current ratings, a relatively low efficiency. Therefore, a practicable solution is to operate several converter stages in parallel to achieve an acceptable total efficiency. Here, a possible solution for such a converter is presented. The input voltage of about 2V has to be converted into a DC-link voltage of 350V, e.g. for solar-inverter applications. The total power to be managed is 200W. In case of a single stage inverter, this leads to about 100A input current (causing peak values in the power switches of up to 200A!). The resulting component stress is very hard and the design is also difficult to handle. To overcome this problem a topology was chosen, which uses several converter switching stages operating in parallel. All these stages can operate at the same transformer core leading to optimal flux exploitation.

Key-Words: - Solar Converter, DC-to-DC Converter, Voltage doubler, Flux-Doubler

1 Introduction

The main disadvantage of the DC-link supply of solar power inverters operating at low DC-input voltages is the extremely high input current. To overcome this, usually several stages must be operated in parallel. Contrary to this, a transformer-based current sharing architecture with voltage doubling rectifier is used in this paper.

1.1 The Basic Converter Topology

The primary (low voltage) side of the proposed converter was realized by the well-known push-pull structure (c.f. Fig. 1) [1,2,3].

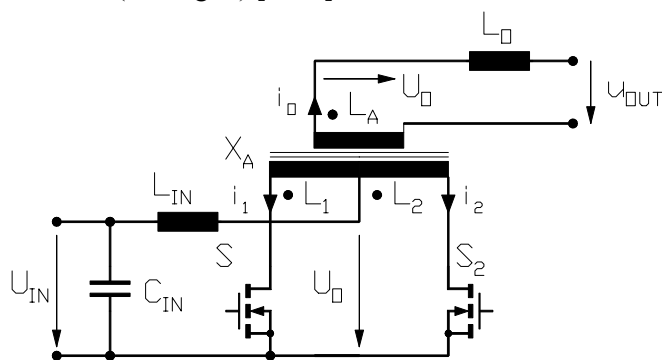


Fig. 1. Basic (push-pull) converter topology

To clarify the operation principle, four different system states can be given (cf. Fig. 2):

- a.) S_1 and S_2 are conducting: the input current i_{IN} rises, no resulting transformer flux
- b.) S_1 opened: positive transformer flux results to positive output voltage

- c.) S_1 and S_2 are conducting: the input current i_{IN} increases, no resulting transformer flux
- d.) S_2 opened: negative transformer flux results to negative output voltage.

An idealized transformer is assumed to explain the basic principle. Therefore, the main-inductor of the transformer (L_M) and the magnetizing losses (represented by R_M) are neglected.

1.2 Operation Principle

As can be seen from Fig. 1, the structure is very similar to the standard boost-converter. A detailed circuit level base simulation was chosen to analyze the component stress.

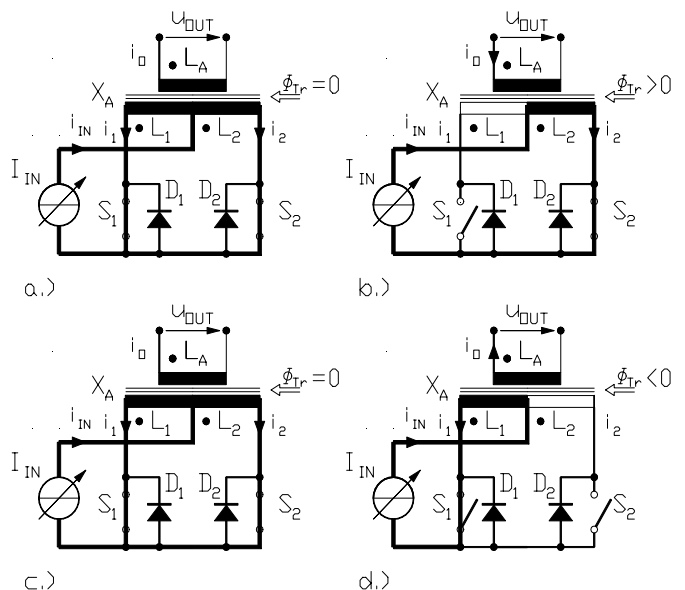


Fig. 2. Operational principle of the converter

For each operation state the system equations can be given:

$$U_{TR}(=U[L_1]) = +U_{IN} \quad (1)$$

$$U_{IN} - U_0 = i_1 \cdot (R_{L1} + R_{L1} + R_O) + \frac{di_1}{dt} (L_{S1} + L_{S1} + L_O) \quad (2)$$

$$i_1 = \frac{U_{IN} - U_{DC}}{R_{L1} + R_{L2} + R_O} \cdot \left(1 - e^{-\frac{R_{L1} + R_{L2} + R_{L_t}}{L_{S1} + L_{S2} + L_O} t} \right) + i_{AB} \cdot e^{-\frac{R_{L1} + R_{L2} + R_{L_t}}{L_{S1} + L_{S2} + L_O} t} \quad (3)$$

$$U_{TR}(=U[L_1]) = -U_{IN} \quad (4)$$

$$-U_{IN} - U_{DC} = i_1 \cdot (R_{L1} + R_{L1} + R_O) + \frac{di_1}{dt} (L_{S1} + L_{S1} + L_O) \quad (5)$$

$$i_1 = -\frac{U_{IN} + U_{DC}}{R_{L1} + R_{L2} + R_O} \cdot \left(1 - e^{-\frac{R_{L1} + R_{L2} + R_{L_t}}{L_{S1} + L_{S2} + L_O} t} \right) + i_{AB} \cdot e^{-\frac{R_{L1} + R_{L2} + R_{L_t}}{L_{S1} + L_{S2} + L_O} t} \quad (6)$$

2 Simulation Results of the Standard Structure

The structure given in Fig. 1 was modeled in PSPICE and simulated. For this simplified breadboard model a 1:32-transformer was used. The simulation results of the topology (input voltage: 12V, load resistance: 1kΩ, duty cycle: 50%) are shown in Fig. 3.

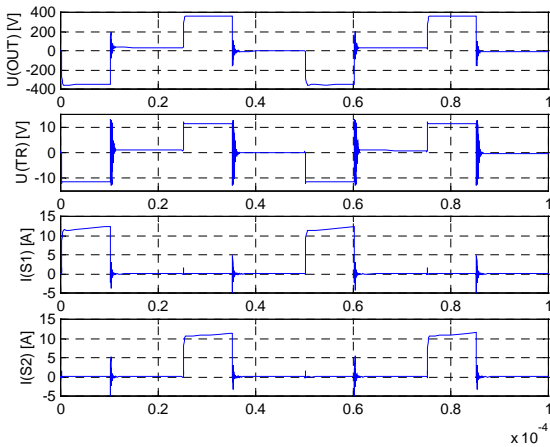


Fig. 3. Simulation: from top to bottom: output voltage, voltage across one primary, current through the switches S₁ & S₂.

For the sake of clarity and to show the influence of the magnetizing current, a transformer ratio of 1:1 is chosen in Figs. 4, 5 & 6. Figure 5 shows the simulation results at no load condition of the converter, while Fig. 6 depicts a 12A load condition (1Ω load). The magnetizing current can be seen clearly in both cases.

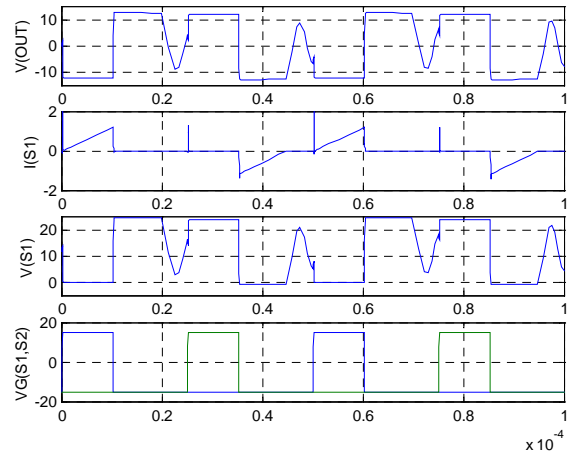


Fig. 4. Simulation from top to bottom: output voltage, transformer current (here magnetizing current), voltage across one switch, control signal of the switches,

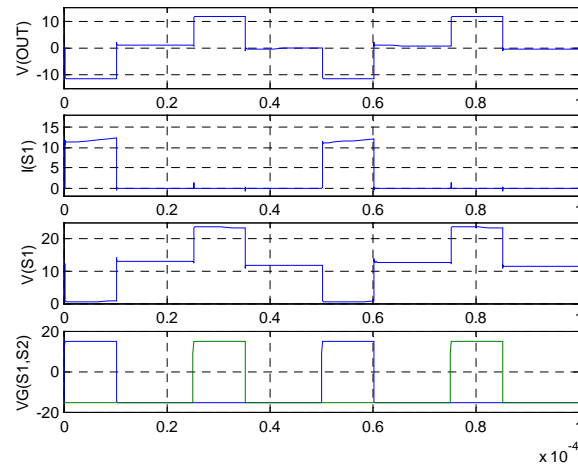


Fig. 5. Simulation from top to bottom: output voltage, transformer current (magnetizing plus transformed load current), voltage across one switch, control signal of the switches. (discontinuous mode).

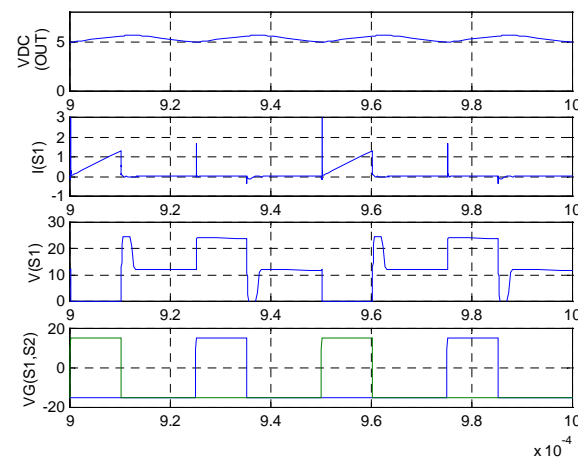


Fig. 6. Simulation from top to bottom: output voltage, switch current (magnetizing plus transformed load current), voltage across one switch, control signal of the switches. (inductive load).

3 The Current Sharing Converter Topology

The basic topology was used to build the converter system given in Fig. 7. Here two stages are operating in parallel. The stages A and B are operated with the same duty-cycle. In case of different supply sources for LA and LB the duty cycle for each converter stage has to be controlled separately to obtain an optimal load sharing. Care must be taken in this case for synchronization of the driving signals.

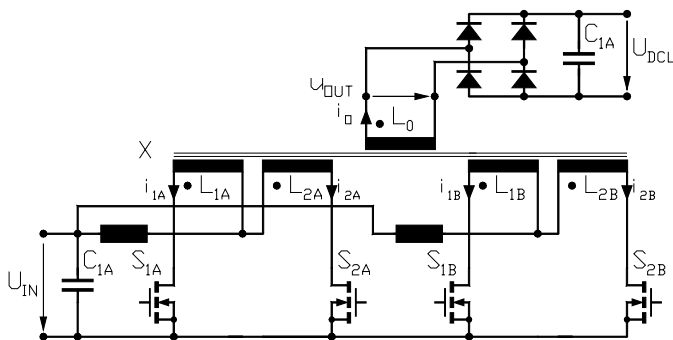


Fig. 7 Current amplifier topology (Flux Doubler), derived converter model

4 Simulation Results of the Current Sharing Topology

As one can see from the simulation results (Figs. 9 & 10), the new topology leads to a current sharing between the stages. The resulting current stress in the power semiconductors is divided by the number of operating stages working in parallel. Here also a winding ratio of 1:1 is used for explanation. In Fig. 8 the no load condition and in Fig. 9 an approximately 12A load case ($R_L=1\Omega$) are shown.

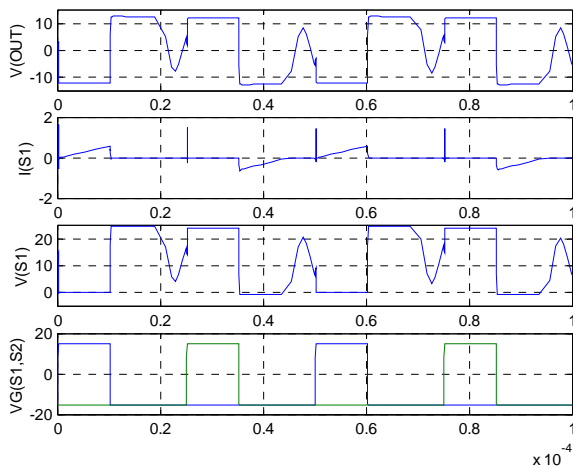


Fig. 8. Simulation from top to bottom: output voltage, transformer current (here magnetizing current), voltage across one switch, control signal of the switches.

A major advantage is the insensitivity of the structure in case of down powered stages or stages operating only at a partial load point.

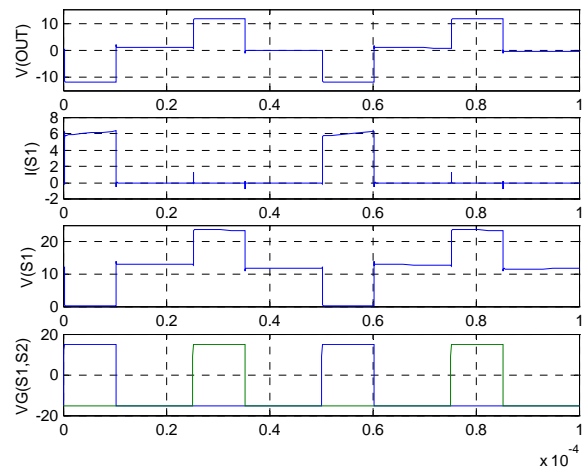


Fig. 9. Simulation from top to bottom: output voltage, transformer current (magnetizing plus transformed load current), voltage across one switch, control signal of the switches.

This is very useful when applied at solar power inverters, where several solar arrays can easily be connected in parallel operating each array at its special MPP (maximum power point).

The resulting efficiency of the solution is therefore much better than a global serial or parallel connection of the arrays.

5 Realization of the Converter

The principal topology given in Fig. 7 uses a simple transformer arrangement realized by an E-core derivate (ELP-64 – in EE-composition) and external high current surface mount power inductors (L_A and L_B)

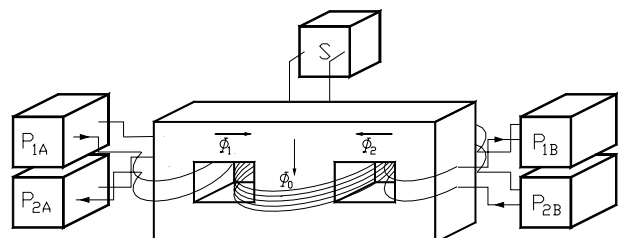


Fig. 10. Inverter topology

As shown in Fig. 10 the arrangement uses converters operating on the left side of a standard E-core and also converters on the right side. As described, the accumulated flux of the transformer is fed through the center leg, where the secondary windings are located, and results in an approximately doubled voltage transfer ratio of this structure in case of symmetry.

When the converters are operated with the same control signals, the flux in the center leg is doubled. This is the normal operation mode. In case of multiple solar arrays, only small differences in the control signal will occur to keep each array-field at MPP.

In case of asymmetric operation, a different state has to be taken into consideration.

Here only one side of the converter is operating. The resulting flux in the center leg is smaller than the flux generated by the source (e.g. left side) depending on the relationship of the magnetic resistances due to the different geometric of the center and the outside legs. Only a part of the generated magnetic flux contributes to the output voltage. In this case the voltage transfer ratio of the converter is reduced.

The current sharing can be managed by operating several converters in parallel on the same leg of the core (e.g. a and b in Fig. 9). In this case the converter current is shared between the single stages. This helps to minimize the current stress in the power semiconductors.

6 Realization of the Transformer

The practical realization of a converter based on two stages as given in Fig. 8 using an E-core transformer is shown in Fig. 11. The primary windings (P_{1A} & P_{1B} , P_{2A} & P_{2B}) are realized by thick copper traces (210 μ m) on a PCB (cf. Fig. 12). The secondary side was realized as a conventional multitrans HF-litz coil on the center leg of the core.

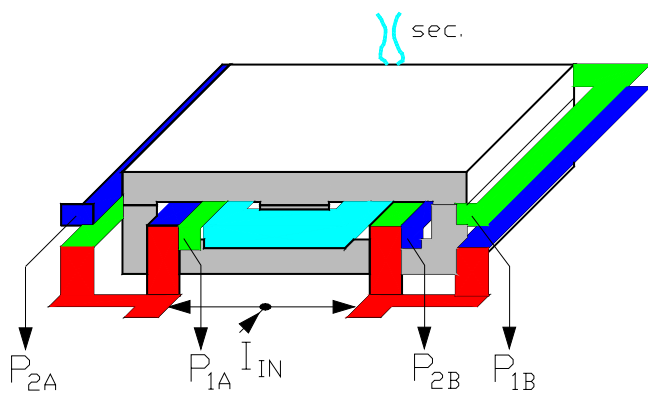


Fig. 11 Transformer schematic

Due to the summation of the magnetic fluxes, the winding voltage on the secondary side is doubled leading to a more effective and compact design.

Another important task is the selection of the rectifier stage. If a center-tapped transformer is used, the voltage ratings of the diodes are more than twice of the nominal output voltage of the converter.

This disadvantage can be overcome by two identical secondary sections connected in series. The disadvantage of increased losses, due to the forward voltage of two

diodes connected in series, is partly compensated by the reduced switching losses (which are proportional to the voltage squared of the series connection). Another possibility to reduce the component stress is the use of a voltage- respectively current doubler output stages [4,5,6]. The resulting design leads to an acceptable efficiency and can help to increase the over-all reliability by lowering the component stress.

7 Realization of the Converter

Figure 13 shows the sample converter. The power transformer was built on one side of the printed circuit board (100 x 60mm), while most electronic components are located on the top-layer. The resulting design gives advantages in cooling and leads to a satisfactory power density.

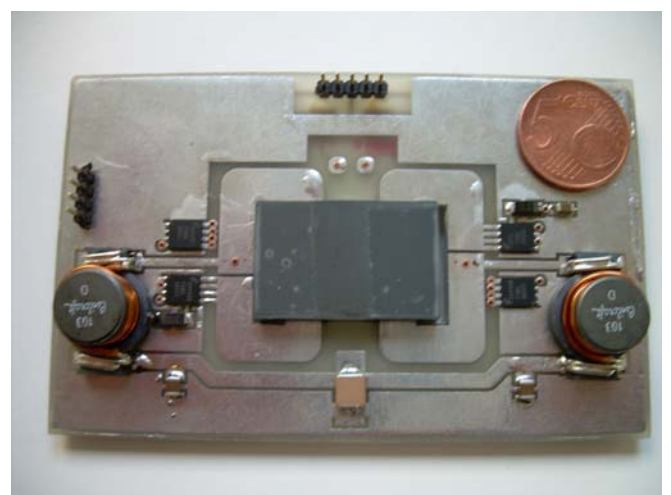
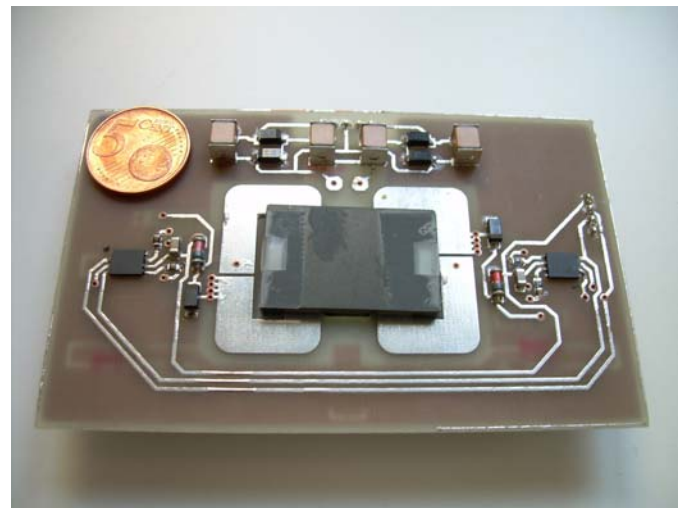


Fig. 12.a,b Bread boarded prototype converter, top view, bottom view

The design excludes the need of active (fan) cooling up to 200W. Due to the very low supply of 2V and the resulting high current ratings in this case thick copper

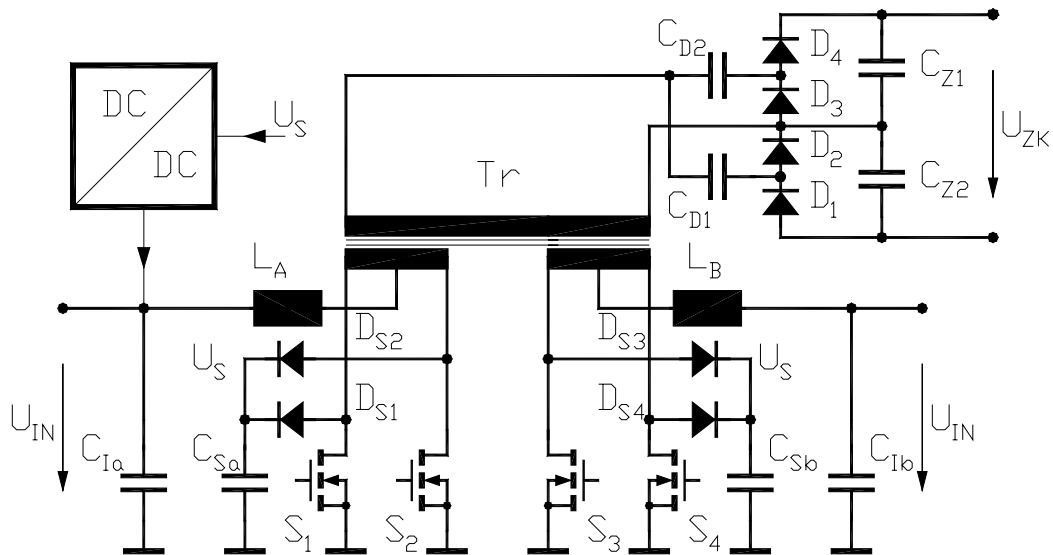


Fig. 13 Schematics of the converter including snubber loss recovery by optional DC-to-DC converter

traces are necessary (210µm). To avoid voltage overshoots and to minimize the leakage inductances a bifilar layout technique is used.

8 Conclusion

The presented converter structure fulfills all requirements of DC-to-DC converters with very low input and high output voltage ratings. The relatively low efficiency, which normally occurs due to the high current ratings, can be overcome by the magnetic current sharing method eliminating the need of a hard parallel operation of several converter stages to achieve an acceptable total efficiency. The used sharing method is also well suited in most applications, where high current ratings have to be maintained. The breadboard sample converter shows a satisfying efficiency for the usage in solar power applications where high efficiency and an excellent reliability are points of major importance. The chosen design gives advantages in cooling and leads to a satisfactory power density. It excludes the need of active (fan) cooling up to an output power of 200W.

Measurement result shows an achievable maximum efficiency of up to 94%

Due to the rather simple structure, the converter is easy to control. It is well suited for digital implementation in an embedded microcontrollers. Modern microcontrollers include most of the peripherals required to implement the full system (ADC, PWM, Timers, etc.). Thus, the solution can be built in a very cheap way, optimal for mass products. On the other hand, the robustness of the design can help to minimize the required computation power, so additional control algorithm can be implemented at the same core (maximum power point tracking, security functions e.g. isolation monitoring on

the DC side, mains impedance surveillance to prevent local operation in mains connected applications).

References:

- [1] Hung, J.-C.; Wu, T.-F.; Tsai, J.-Z.; Tsai, C.-T.; Chen, Y.-M.: An active-clamp push-pull converter for battery sourcing applications. Twentieth Annual IEEE Applied Power Electronics Conference and Exposition, APEC 2005. Volume 2, March 6-10, 2005, pp.1186-1192.
- [2] De Aragao Filho, W.C.P.; Barbi, I.: A comparison between two current-fed push-pull DC-DC converters-analysis, design and experimentation. 18th International Telecommunications Energy Conference INTELEC '96. Oct.6-10, 1996, pp.313-320
- [3] Tseng, S.-Y.; Wu, T.-F.; Chen, S.-S.: Soft-switching push-pull converter associated with a full-bridge inverter for caprahircas stunning applications. Twenty-First Annual IEEE Applied Power Electronics Conference and Exposition, APEC '06. March 19-23, 2006, pp.1523-1529
- [4] Xiaolin Gao; Ayyanar, R.: A high-performance, integrated magnetics scheme for buck-cascaded push-pull converter. IEEE Power Electronics Letters, Volume 2, Issue 1, March 2004, pp.29-33
- [5] Peng X., Qiaoqiao W., Pit-Leong W., Lee F.C.: A Novel Integrated Current Doubler Rectifier. Fifteenth Annual IEEE Applied Power Electronics Conference and Exposition, APEC 2000, Vol. 2, pp. 735 -740.
- [6] H. Kiyotake, H. Okada, K. Ishizaka, R. Itoh: "Single-phase voltage-doubler rectifier using a capacitive energy storage/transfer mechanism", IEE Proceedings of Electric Power Applications, Volume 150, Issue 1, Jan. 2003, pp.:81 – 87.